REVIEW OF THE STRUCTURAL AND MECHANICAL PROPERTIES OF GALLIUM NITRIDE (GaN) USING THE ENERGY STRAIN METHOD: AN ABINITO CALCULATION

BY

OSEMWENGIE EMMANUEL ETINOSA

(B.Sc Pure Physics)

MATRIC.NO. PSC1809287

DEPARTMENT OF PHYSICS,

FACULTY OF PHYSICAL SCIENCES,

UNIVERSITY OF BENIN

SEPTEMBER, 2023

REVIEW OF THE MECHANICAL PROPERTIES OF GALLIUM NITRIDE (GaN) USING THE ENERGY STRAIN METHOD: AN ABINITO CALCULATION

BY

OSEMWENGIE EMMANUEL ETINOSA

(B.Sc Pure Physics)

MATRIC.NO. PSC1809287

A PROJECT SUBMITTED TO THE DEPARTMENT OF PHYSICS,
FACULTY OF PHYSICAL SCIENCES, UNIVERSITY OF BENIN,
BENIN CITY, EDO STATE, NIGERIA

IN PARTIAL FULFILMENT OF THE REQUIREMENTS OF THE AWARD OF
BACHELOR OF SCIENCE DEGREE IN PHYSICS

SEPTEMBER, 2023

CERTIFICATION

I hereby certify that I approve the following research essay adequately performed in the Department of Physics under supervision in scope and quality for the partial fulfilment of (B.Sc. Hons) Degree in Physics.

PROF. O.D OSAHON DATE
(Head of Department)

DR. M.I. BABALOLA DATE
(Project Supervisor)

EXTERNAL EXAMINER DATE

DEDICATION

I dedicate my project work to God Almighty for His Grace, Divine guidance and Support through my stay in the University of Benin. And also I want to say a big thanks to my parents, my siblings for their love and support.

CERTIFICATION OF DISSERTATION OF PLAGIARISM

We undersigned, attest and declare that the dissertation of Osemwengie Emmanuel Etinosa titled "First Principle calculation of the Structural and Mechanical properties of (GaN) Gallium Nitride in Wurtzite crystal structure" has successfully passed the anti-plagiarism test and does not violate any copyright© regulations.

PROF. O.D OSAHON DATE
(Head of Department)

DR. M.I. BABALOLA DATE
(Project Supervisor)

ACKNOWLEDGEMENT

I wish to express my outmost gratitude to God Almighty for his wisdom, understanding and mercy and also his grace to successfully complete this project work.

My special thanks to my parents (Mr. & Mrs. OSEMWENGIE) for their encouragement, love, care, financial support and their assistance to me.

Secondly, I wish to appreciate my project supervisor Doctor M.I. BABALOLA for his immense guidance and support in making my project research and experimentation a success.

I would also like to appreciate my uncle, my aunt, friends, course mates, and loved ones for their emotional support and encouragement throughout the duration of my project work.

TABLE OF CONTENTS

CHAPTER ONE

CHAPTER TWO

CHAPTER THREE

Methodology

LIST OF TABLES

LIST OF FIGURES

ABSTRACT

Several methods have been employed to calculate the mechanical properties of GaN with reliable results. In this work, we employed the energy strain method from first-principles calculation to review the structural and mechanical properties of GaN. From our results, we observed that there is agreement in some of the elastic constants when compared with literature review.

CHAPTER ONE

INTRODUCTION

1.0 SEMICONDUCTORS

The history of the understanding of semiconductors begins with experiments on the electrical properties of materials. The properties of the time-temperature coefficient of resistance, rectification, and light-sensitivity were observed starting in the early 19th century.

Thomas Johann Seeback was the first to notice an effect due to semiconductors, in 1821. In 1833, Michael Faraday reported that the resistance of specimens of silver sulfide decreases when they are heated. This is contrary to the behavior of metallic substances such as copper. In 1874, Karl Ferdinand Braun observed conduction and rectification in metallic sulfides, although this effect had been discovered much earlier by Peter Munck af Rosenschold writing for Annalen der Physik und Chemie in 1835 (Morris, Peter Robin, 1990), and Arthur Schuster found that a copper oxide layer on wires has rectification properties that ceases, when the wires are cleaned. William Grylls Adams and Richard Evans Day observed the photovoltaic effect in selenium in 1876 (Lidia Lukasiak and Andrej Jakubowski, 2010).

Thus, a Semiconductor is a material which has an electrical conductivity value falling between that of a conductor, such as copper, and an insulator such as glass. Its resistivity falls as its temperature rises; metals behave the opposite way. Its conducting properties may be altered in useful ways by introducing impurities ("doping") into the crystalline structure. When two differently doped regions exist in the same crystal, a semiconductor junction is created. The behavior of charge carriers, which include electrons, ions, and electron holes, at these junctions is the basis of diodes, transistors and most modern electronics. Semiconductor devices can display a range of different useful properties, such as passing current more easily in one direction than the other, showing variable resistance, and having sensitivity to light or heat. Because the electrical properties of a semiconductor material can be modified by doping and by the application of electrical fields or light, devices made from semiconductors can be used for amplification, switching, and energy conversion.

The modern understanding of the properties of a semiconductor relies on quantum physics to explain the movement of charge carriers in a crystal lattice (Feynman, Richard). Doping greatly increases the number of charge carriers within the crystal. When a doped semiconductor contains free holes, it is called “p-type”, and when it contains free electrons, it is known as “n-type”. The semiconductor materials used in electronic devices are doped under precise conditions to control the concentration and regions of p- and n-type dopants. A single semiconductor device crystal can have many p- and n-type regions; the p-n junctions between these regions are responsible for the useful electronic behavior. Using a hot-point probe, one can determine quickly whether a semiconductor sample is p- or n-type (ecee.colorado.edu, 2021).

A few of the properties of semiconductor materials were observed throughout the mid-19th and first decades of the 20th century. The first practical application of semiconductors in electronics was the 1904 development of the cat's-whisker detector, a primitive semiconductor diode used in early radio receivers. Developments in quantum physics led in turn to the invention of the transistor in 1947 (William Shockley, 1950) and the integrated circuit in 1958.

Unlike in conventional semiconductors like silicon, gallium arsenide, and silicon carbide, where electrons and holes are typically described as non-relativistic particles exhibiting parabolic energy-momentum dispersions (Charles Kittel, 1996), (M.A. Green, 1990) recent discoveries in novel semiconductors, such as the quasi-Dirac and semi-Dirac materials proposed in the Tang-Dresselhaus Theory by Shuang Tang and Mildred Dresselhaus at the Massachusetts Institute of Technology, have revealed the existence of electrons and holes with relativistic effects (Shuang Tang and Mildred Dresselhaus, 2012). These new materials exhibit intriguing properties that differ from the behavior of traditional semiconductors for developing the next-generation computer chips and energy converters.

1.1 TYPES OF SEMICONDUCTORS

1.1.1 INTRINSIC SEMICONDUCTOR

An intrinsic (pure) semiconductor, also called an undoped semiconductor or i-type semiconductor, is a pure semiconductor without any significant dopant species present. The number of charge carriers is therefore determined by the properties of the material itself instead of the amount of impurities. In intrinsic semiconductors the number of excited electrons and the number of holes are equal: n = p. This may be the case even after doping the semiconductor, though only if it is doped with both donors and acceptors equally. In this case, n = p still holds, and the semiconductor remains intrinsic, though doped. This mean that some conductors are both intrinsic as well as extrinsic but only if n (electron donor dopant/excited electrons) is equal to p (electron acceptor dopant/vacant holes that act as positive charges) (M. Simon Sze, 1981) (Charles Kittel, 1996)

1.1.2 EXTRINSIC SEMICONDUCTOR

An extrinsic semiconductor is one that has been doped; during manufacture of the semiconductor crystal a trace element or chemical called a doping agent has been incorporated chemically into the crystal, for the purpose of giving it different electrical properties than the pure semiconductor crystal, (an intrinsic semiconductor). In an extrinsic semiconductor it is these foreign dopant atoms in the crystal lattice that mainly provide the charge carriers which carry electric current through the crystal. The doping agents used are of two types, resulting in two types of extrinsic semiconductor. An extrinsic semiconductor which has been doped with electron donor atoms is called an n-type semiconductor, because the majority of charge carriers in the crystal are negative electrons. In the n-type semiconductor, the majority carriers are the electrons while the minority carriers are holes An electron acceptor dopant is an atom which accepts an electron from the lattice, creating a vacancy where an electron should be called a hole which can move through the crystal like a positively charged particle. An extrinsic semiconductor which has been doped with electron acceptor atoms is called a p-type semiconductor, because the majority of charge carriers in the crystal are positive holes (A. Donald Neaman, 2003).

1.2 PROPERTIES OF SEMICONDUCTORS

1.2.1 ELECTRICAL PROPERTIES

Semiconductors are a class of materials that have electrical properties that lie between those of conductors(such as metals) and insulators (such as non metals). Below are some of the key electrical properties of semiconductors:

1.2.1.1 BAND GAP

In semiconductors , electrons are confined to a number of bands of energy, and forbidden from other regions because there are no allowable electronic states for them to occupy. The term “band gap” refers to the energy difference between the top of the valence band and the bottom of the conduction band. Electrons are able to jump from one band to another. The distinction between semiconductors and insulators is a matter of convention. One approach is to think of semiconductors as a type of insulator with a narrow band gap. Insulators with larger band gap, usually greater than 4eV (V.Suresh Babu, 2010), are not considered semiconductors and generally do not exhibit semiconductive behavior under practical conditions. The band-gap energy of semiconductors tends to decrease with increasing temperature. When temperature increases, the amplitude of atomic vibrations increase, leading to larger interatomic spacing. The interaction between the lattice phonons and the free electrons and holes will also affect the band gap to a smaller extent. (Hilmi Unlu, 1992).

1.2.1.2 CARRIER MOBILITY

In solid-state physics, the electron mobility characterises how quickly an electron can move through a metal or semiconductor when pulled by an electric field. There is an analogous quantity for holes, called hole mobility. The term carrier mobility refers in general to both electron and hole mobility

1.2.1.3 CONDUCTIVITY

In semiconductors, electrical conductivity is a crucial property that plays a central role in their operation as electronic devices. In Intrinsic semiconductors, the conductivity is at its natural level even at room temperature. In extrinsic semiconductors, doping enhances conductivity. This results in the majority carriers(electrons or holes) dominating the conductivity, significantly increasing the conductivity compared to intrinsic conditions.(G.B. Streetman and S.K Banerjee, 2005) (R.F. Pierret, 1996)

1.2.2 STRUCTURAL PROPERTIES

The structural properties or crystal structure is a description of the ordered arrangement of atoms, ions or molecules in a crystalline material (J.R. Hook and H.E. Hall, 2010). Ordered structures occur from the intrinsic nature of the constituent particles to form symmetric patterns that repeat.

The smallest group of particles in the material that constitutes this repeating pattern is the unit cell of the structure. The unit cell completely reflects the symmetry and structure of the entire crystal, which is built up by repetitive translation of the unit cell along its principal axes. The translation vectors define the nodes of the Bravais lattice (J.R. Hook and H.E. Hall, 2010)..

The lengths of the principal axes, or edges, of the unit cell and the angles between them are the lattice constants, also called lattice parameters or cell parameters. The symmetry properties of the crystal are described by the concept of space groups.

1.2.3 TYPES OF CRYSTAL STRUCTURES

1.2.3.1 TRICLINIC STRUCTURE

In crystallography, the triclinic (or anorthic) crystal system is one of the 7 crystal systems. A crystal system is described by three basis vectors. In the triclinic system, the crystal is described by vectors of unequal length, as in the orthorhombic system. In addition, the angles between these vectors must all be different and may not include 90°.

The triclinic lattice is the least symmetric of the 14 three-dimensional Bravais lattices. It has (itself) the minimum symmetry all lattices have: points of inversion at each lattice point and at 7 more points for each lattice point: at the midpoints of the edges and the faces, and at the center points. It is the only lattice type that itself has no mirror planes (E. Prince, ed, 2006).

1.2.3.2 MONOCLINIC STRUCTURE

In the monoclinic system, the crystal is described by vectors of unequal lengths, as in the orthorhombic system. They form a parallelogram prism. Hence two pairs of vectors are perpendicular (meet at right angles), while the third pair makes an angle other than 90°. Two monoclinic Bravais lattices exist: the primitive monoclinic and the base-centered monoclinic. For the base-centered monoclinic lattice, the primitive cell has the shape of an oblique rhombic prism; (Hahn, 2002)

1.2.3.3 ORTHORHOMBIC STRUCTURE

Orthorhombic lattices result from stretching a cubic lattice along two of its orthogonal pairs by two different factors, resulting in a rectangular prism with a rectangular base (*a* by *b*) and height (*c*), such that *a*, *b*, and *c* are distinct. All three bases intersect at 90° angles, so the three lattice vectors remain mutually orthogonal.(Hahn, 2002)

1.2.3.4 TETRAGONAL STRUCTURE

The tetragonal crystalline structure contains three axes, and the central axis has a different length (either shorter or longer than others). The other two axes are in the same plane and have the same lengths. The tetragonal crystal shape includes double and 8-sided pyramids, 4-sided prism, pyrite, and trapezohedrons. A tetragonal system has simple and body-centred tetragonal cells, and the Bravais lattice follows the given relation:

- a, b are equal but not equal to c
- α, β and γ equals to 90 degree

Tetragonal crystal system examples are for the simple cells and body-centred cells structures. The typical examples of tetragonal crystal system are Titanium dioxide and Stannic Oxide.

Note: Here, a, b, and c denotes the dimensions of unit cells and α, β, and γ denotes the angles corresponding in the unit cells. (Vendantu, 2023)

1.2.3.5 TRIGONAL AND HEXAGONAL STRUCTURES

In crystallography, the hexagonal crystal family is one of the six crystal families, which includes two crystal systems (hexagonal and trigonal) and two lattice systems (hexagonal and rhombohedral). While commonly confused, the trigonal crystal system and the rhombohedral lattice system are not equivalent (Hahn, Theo, ed., 2005). In particular, there are crystals that have trigonal symmetry but belong to the hexagonal lattice (such as α-quartz).

The hexagonal crystal family consists of the 12 point groups such that at least one of their space groups has the hexagonal lattice as underlying lattice, and is the union of the hexagonal crystal system and the trigonal crystal system (James Dana and Cornelius Hurlbert, 1959). There are 52 space groups associated with it, which are exactly those whose Bravais lattice is either hexagonal or rhombohedral..

1.2.3.6 CUBIC STRUCTURE

In crystallography, the cubic (or isometric) crystal system is a crystal system where the unit cell is in the shape of a cube. This is one of the most common and simplest shapes found in crystals and minerals.

There are three main varieties of these crystals:

- Primitive cubic (abbreviated *cP* and alternatively called simple cubic)
- Body-centered cubic (abbreviated *cI* or bcc)
- Face-centered cubic (abbreviated *cF* or fcc)

1.2.4 MULTI-ELEMENT STRUCTURES

1.2.4.1 WURTZITE STRUCTURE

Wurtzite is a zinc and iron sulfide mineral with the chemical formula (Zn,Fe)S, a less frequently encountered structural polymorph form of sphalerite. The iron content is variable up to eight percent (Harry Berman et al, 1944). It is trimorphous with matraite and sphalerite (S. Graeser, 2011).

The Wurtzite crystal structure is referred to by the Strukturbericht designation B4 and the Pearson symbol hP4. The corresponding space group is No. 186 (in International Union of Crystallography classification) or $P6_3mc$ (in Hermann–Mauguin notation). The Hermann-Mauguin symbols in $P6_3mc$ can be read as follows (Peter B. Hitchcock, 1988):

- 6_3.. : a six fold screw rotation around the c-axis
- .m. : a mirror plane with normal {100}
- ..c : glide plane in the c-directions with normal {120}.

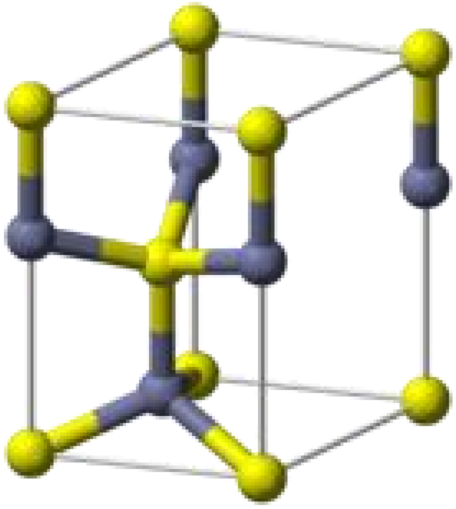

Figure 1.1: Representation of Wurtzite unit cell

Among the compounds that can take the wurtzite structure are wurtzite itself (ZnS with up to 8% iron instead of zinc), silver iodide (AgI), zinc oxide (ZnO), cadmium sulfide (CdS), cadmium selenide (CdSe), silicon carbide (α-SiC), gallium nitride (GaN), aluminium nitride (AlN), boron nitride (w-BN) and other semiconductors (Atsushi Togo, et al, 2015). In most of these compounds, wurtzite is not the favored form of the bulk crystal, but the structure can be favored in some nanocrystal forms of the material.

Each of the two individual atom types forms a sublattice which is hexagonal close-packed (HCP-type). When viewed all together, the atomic positions are the same as in lonsdaleite (hexagonal diamond). Each atom is tetrahedrally coordinated. The structure can also be described as an HCP lattice of zinc with sulfur atoms occupying half of the tetrahedral voids or vice versa.

1.2.5 MECHANICAL PROPERTIES

1.2.5.1 ELASTIC MODULUS

An elastic modulus (also known as modulus of elasticity) is the unit of measurement of an object's or substance's resistance to being deformed elastically (i.e., non-permanently) when a stress is applied to it. The elastic modulus of an object is defined as the slope of its stress-strain curve in the elastic deformation region (Donald Askeland and Pradeep Phule, 2006). A stiffer material will have a higher elastic modulus. An elastic modulus has the form:

$$\delta = \text{stress}/\text{strain} \qquad (1.1)$$

where stress is the force causing the deformation divided by the area to which the force is applied and strain is the ratio of the change in some parameter caused by the deformation to the original value of the parameter.

Since strain is dimensionless, the units of **δ** will be the same as the units of stress (Ferdinand P. Beer et al, 2009).

1.2.5.1.1 TYPES OF ELASTIC MODULUS

Specifying how stress and strain are to be measured, including directions, allows for many types of elastic moduli to be defined. The four primary ones are:

1. Young's modulus (*E*) describes tensile and compressive elasticity, or the tendency of an object to deform along an axis when opposing forces are applied along that axis; it is defined as the ratio of tensile stress to tensile strain. It is often referred to simply as the elastic modulus.
2. The shear modulus or modulus of rigidity (*G* or Lamé second parameter) describes an object's tendency to shear (the deformation of shape at constant volume) when acted upon by opposing forces; it is defined as shear stress over shear strain. The shear modulus is part of the derivation of viscosity.
3. The bulk modulus (*K*) describes volumetric elasticity, or the tendency of an object to deform in all directions when uniformly loaded in all directions; it is defined as volumetric stress over volumetric strain, and is the inverse of compressibility. The bulk modulus is an extension of Young's modulus to three dimensions.
4. Flexural modulus (E_{flex}) describes the object's tendency to flex when acted upon by a moment.

Two other elastic moduli are Lamé's first parameter, λ, and P-wave modulus, M, as used in table of modulus comparisons given below references. Homogeneous and isotropic (similar in all directions) materials (solids) have their (linear) elastic properties fully described by two elastic moduli, and one may choose any pair.

1.3 AIM AND OBJECTIVES

AIM

To study the mechanical and structural properties of GaN (Gallium Nitride) in Wurtzite structure

OBJECTIVES

The objective of this work are to employ first principle calculation to study the;

- Structural properties of GaN in Wurtzite crystal structure
- Mechanical properties of GaN in Wurtzite crystal structure

CHAPTER TWO

LITERATURE REVIEW

2.0 GALLIUM NITRIDE (GAN)

Gallium nitride (GaN) is a binary III/V direct bandgap semiconductor commonly used in blue light-emitting diodes since the 1990s. The compound is a very hard material that has a Wurtzite crystal structure. Its wide band gap of 3.4 eV affords it special properties for applications in optoelectronic (A. Di Carlo, 2001) (Y. Arakawa, 2002) high-power and high-frequency devices. For example, GaN is the substrate which makes violet (405 nm) laser diodes possible, without requiring nonlinear optical frequency-doubling.

Its sensitivity to ionizing radiation is low (like other group III nitrides), making it a suitable material for solar cell arrays for satellites. Military and space applications could also benefit as devices have shown stability in high radiation environments.(Alexander Lidow et al, 2011).

GaN is a very hard (Knoop hardness 14.21 GPa), mechanically stable wide-bandgap semiconductor material with high heat capacity and thermal conductivity. (I. Akansaki and H. Amano, 1997). In its pure form it resists cracking and can be deposited in thin film on sapphire or silicon carbide, despite the mismatch in their lattice constants (I. Akansaki and H. Amano, 1997). GaN can be doped with silicon (Si) or with oxygen (C. Wetzel et al, 1996) to n-type and with magnesium (Mg) to p-type (H. Amano et al, 1989). However, the Si and Mg atoms change the way the GaN crystals grow, introducing tensile stresses and making them brittle (S. Terao et al, 2001). Gallium nitride compounds also tend to have a high dislocation density, on the order of 10^8 to 10^{10} defects per square centimeter (Paul Preuss, 2000).

2.1 PROPERTIES OF GAN

2.1.1 BULK MODULUS

The bulk modulus (K or B) of a substance is a measure of the resistance of a substance to bulk compression. It is defined as the ratio of the infinitesimal pressure increase to the resulting relative decrease of the volume.

It is expressed mathematically as:

$$K = -V\frac{dP}{dV} \qquad (2.1)$$

Where P denotes Pressure, V denotes initial volume, dP/dV is the derivation of pressure with respect to volume.

The bulk modulus of GaN has been measured and calculated using different techniques and calculations. It was calculated to be approximately to be 207 Gpa (Kim et al, 1997).

2.1.2 ELASTIC CONSTANTS

The elastic constants of GaN determines the strength of the material. The elastic constants $C_{11}, C_{12}, C_{13}, C_{33}, C_{44}, C_{66}$ determine the mechanical properties of the material.

Other properties of GaN include:

- The molar mass of GaN 83.730g/mol (M. William Hayden, 2011)
- Appearance: yellow powder
- The density of GaN is 6.1g/cm^3 (M. William Hayden, 2011)
- Melting point >1600^{o}c (Kenji Harafuji et al, 2004)

- The solubility in water of the compound, GaN, is that it is insoluble (M. Corey Foster et al, 2013)
- Band gap: 3.4 eV (300K, direct)
- Electron mobility: 1500cm^2/(VS) (300K) (Johan Strydom et al, 2019)
- Thermal conductivity: 1.3W/(cm.K) (300K) (Christian Mion, 2005)

Calculations on the mechanical properties (elastic constants) of GaN have been carried out numerous times using different methods. The table below shows Bulk modulus, B and elastic constants in (Gpa) for wurtzite GaN carried out using different experiments.

Table 2.1: Bulk modulus B, and the elastic constants C_{11} , C_{12}, C_{13}, C_{33}, C_{44} and C_{66} (Gpa) for GaN in Wurtzite.

Structure (GaN)	**B (GPa)**	C_{11}	C_{12}	C_{13}	C_{33}	C_{44}	C_{66}
DFT	207	367	135	98	409	98	116
Expt[a]	207	346	148	105	389	76	99
Expt[b]	202	367	135	103	405	95	116

[a] *DFT(LDA) calculation by Kim et al.*

[b] *DFT(LDA) calculation by Wright.*

2.2 APPLICATIONS OF GAN

- **Nanoscales:** GaN nanotubes and nanowires are proposed for applications in nanoscale electronics, optoelectronics and biochemical-sensing applications (Chao Zhao et al, 2019)

- **Spintronics potentials:** When doped with a suitable transition metal such as manganese, GaN is a promising spintronics material (magnetic semiconductors). (H. Morkoc et al, 1994)
- **LEDS and lasers:** GaN-based violet laser diodes are used to read Blu-ray Discs. The mixture of GaN with In (InGaN) or Al (AlGaN) with a band gap dependent on the ratio of In or Al to GaN allows the manufacture of light-emitting diodes (LEDs) with colors that can go from red to ultra-violet. (H. Morkoc et al, 1994)
- **Radars:** They are also utilized in military electronics such as active electronically scanned array radars. (Northrop Grumman, 2011).

CHAPTER THREE

METHODOLOGY

3.0 DENSITY FUNCTIONAL THEORY

Density-functional theory (DFT) is a computational quantum mechanical modelling method used in physics, chemistry and material science to investigate the electronic structure (or nuclear structure) (principally the ground state) of many-body systems, in particular atoms, molecules, and the condensed phases. Using this theory, the properties of a many-electron system can be determined by using functionals, i.e. functions of another function. In the case of DFT, these are functionals of the spatially dependent electron density. DFT is among the most popular and versatile methods available in condensed-matter physics, computational physics, and computational chemistry.

In the context of computational materials science, *ab initio* (from first principles) DFT calculations allow the prediction and calculation of material behavior on the basis of quantum mechanical considerations, without requiring higher-order parameters such as fundamental material properties. In contemporary DFT techniques the electronic structure is evaluated using a potential acting on the system's electrons. This DFT potential is constructed as the sum of external potentials V_{ext}, which is determined solely by the structure and the elemental composition of the system, and an effective potential V_{eff}, which represents interelectronic interactions. Thus, a problem for a representative supercell of a material with n electrons can be studied as a set of n one-electron Schrödinger-like equations, which are also known as Kohn–Sham equations. (D. A. H., Hanaor, et al 2012)

3.1 QUANTUM ESPRESSO

Quantum ESPRESSO is a suite for first-principles electronic-structure calculations and materials modeling, distributed for free and as free software under the GNU General Public License. It is based on density-functional theory, plane wave basis sets, and pseudopotentials (both norm-conserving and ultrasoft). ESPRESSO is an acronym for opEn-Source Package for Research in Electronic Structure, Simulation, and Optimization. (P. Glannozzi, S. Baroni, et al, 2009) (P. Glannozzi, O. Andreussi, et al, 2017).

The core plane wave DFT functions of QE are provided by the PWscf component (PWscf previously existed as an independent project). PWscf (Plane-Wave Self-Consistent Field) is a set of programs for electronic structure calculations within density functional theory and density functional perturbation theory, using plane wave basis sets and pseudopotentials. The basic packages include Pwscf, which solves the self-consistent Kohn-Sham equations, obtained for a periodic solid, CP to carry out Car-Parrinello molecular dynamics, and PostProc, which allows data analysis and plotting.

3.1.1 USES OF QUANTUM ESPRESSO

Quantum espresso can be used to perform the following functions:

- Structural optimization
- Ground state calculations
- Transitions states and minimum energy paths
- Ab initio molecular dynamics: Car-Parrinello and Born-Oppenheimer MD
- Quantum import
- Generation of pseudopotentials

3.1.2 COMPUTATION

PWscf is included in the core Quantum ESPRESSO distribution. Instruction on how to install it can be found in the general documentation (User'sGuide) for Quantum ESPRESSO. Typing make pw from the main Quantum ESPRESSO directory or make from the PW/ sub directory produces the pw.x executable in PW/src and a link to the bin/directory. In addition,the following gutility programs, and related links in bin/,are produced in PW/src:

- dist . x symbolic link to pw.x : reads input data for PWscf , calculates distances and angles between atoms in a cell,taking into account periodicity, and in PW/tools:
- kpoints.x produces lists of k-points
- ibrav2cell.x and cell2ibrav.x convert from variables used in Quantum ESPRESSO to specify the unit cell to primitive lattice translations, and vice versa
- scanibrav.x works as cell2ibrav.x but tries to figure out whether the axis are rotated with respect to those assumed by Quantum ESPRESSO

The other auxiliary codes contain their own documentation in the source files.

3.1.3 INPUT DATA

Input data is organized as several name lists, followed by other fields ("cards") introduced by keywords. The name lists are

&CONTROL: general variables controlling the run

&SYSTEM: structural information on the system under investigation &ELECTRONS: electronic variables: self-consistency, smearing &IONS(optional): ionic variables: relaxation, dynamics &CELL(optional):variable-cell optimization or dynamics

Optional name list may be omitted if the calculation to be performed does not require them.

This depends on the value of variable calculation in name list &CONTROL. Most variables in name lists have default values. Only the following variables in &SYSTEM must always be specified:

nat(integer) number of atoms in the unit cell

ntyp(integer) number of types of atoms in the unit cell

ecutwfc(real) kinetic energy cutoff(Ry) for wave functions.

Plus the variables needed to describe the crystal structure, e.g.: ibrav(integer) Bravais-lattice index ; celldm(real, dimension 6)

After the name lists, you have several fields ("cards") introduced by keywords with self explanatory names: ATOMIC_SPECIES; ATOMIC_POSITIONS; K_POINTS; CELL_PARAMETERS (optional); OCCUPATIONS (optional)

3.2 ELASTIC CONSTANTS CALCULATIONS OF GAN

The elastic constants of solids give important information on their mechanical and dynamical properties. These parameters provide a link between the mechanical and dynamic behavior of crystals, and may be used as a means of probing the inter-atomic forces. They provide information on the stability and stiffness of materials.

The theoretical elastic constants are calculated from the energy variation by applying small strains to the equilibrium lattice configuration. The lattice energy of a solid under strain is given by:

$$\Delta E = \frac{V}{2} \sum_{i=1}^{6} \sum_{j=1}^{6} C_{ij} e_i e_j$$

where V is the volume of the undistorted lattice cell, ΔE is the energy increment from the strain with vector e = $(e_1, e_2, e_3, e_4, e_5, e_6)$, and C is the matrix of the elastic constants. For hexagonal phases, there are five independent elastic constants, $C_{11}, C_{12}, C_{13}, C_{33}, C_{44}$. Its primitive vectors are defined as

$$\begin{pmatrix} a_1 \\ a_2 \\ a_3 \end{pmatrix} = \begin{pmatrix} 0 & \frac{a}{2} & \frac{a}{2} \\ \frac{a}{2} & 0 & \frac{a}{2} \\ \frac{a}{2} & \frac{a}{2} & 0 \end{pmatrix}$$

Where *a* is the lattice constant. The primitive vectors of the hexagonal phase are defined by

$$\begin{pmatrix} a_1 \\ a_2 \\ a_3 \end{pmatrix} = \begin{pmatrix} 0 & 0 & 0 \\ -\frac{1}{2} & \frac{\sqrt{3}}{2} & 0 \\ 0 & 0 & \frac{c}{a} \end{pmatrix}$$

Where *a* and *c* are lattice constants. The primitive vectors a_i (*i* = 1, . . . , 3) are transformed to the new vectors under strain by

$$\begin{pmatrix} a_1^{'} \\ a_2^{'} \\ a_3^{'} \end{pmatrix} = \begin{pmatrix} a_1 \\ a_2 \\ a_3 \end{pmatrix} . (I + \varepsilon)$$

Where *ε* is the strain tensor. This links with the strain vector *e* by

$$\varepsilon = \begin{pmatrix} e_1 & \frac{e_6}{2} & \frac{e_5}{2} \\ \frac{e_6}{2} & e_2 & \frac{e_4}{2} \\ \frac{e_5}{2} & \frac{e_4}{2} & e_3 \end{pmatrix}$$

Therefore,

$$\begin{pmatrix} a_1' \\ a_2' \\ a_3' \end{pmatrix} = \begin{pmatrix} e_1+1 & \frac{e_6}{2} & \frac{e_5}{2} \\ [-\frac{1}{2}(e_1+1)+\sqrt{3}\frac{e_6}{4}] & [-\frac{e_6}{4}+\frac{\sqrt{3}}{2}(e_2+1)] & [-\frac{e_5}{4}+\sqrt{3}\frac{e_4}{4}] \\ \frac{c}{a}.\frac{e_5}{2} & \frac{c}{a}.\frac{e_4}{2} & \frac{c}{a}(e_3+1) \end{pmatrix}$$

Firstly, one applies the strain *e* = (δ, δ, 0, 0, 0, 0) to calculate $C_{11} + C_{12}$:

$$D1 = \begin{pmatrix} 1+\delta & 0 & 0 \\ -\frac{1}{2}(1+\delta) & \frac{\sqrt{3}}{2}(1+\delta) & 0 \\ 0 & 0 & \frac{c}{a} \end{pmatrix}$$

$$\frac{\Delta\mathrm{E}}{V} = (C_{11} + C_{12})\delta^2$$

Then $C_{11} - C_{12}$ is calculated using the strain *e* = (0, 0, 0, 0, 0, δ) :

$$D2 = \begin{pmatrix} 1 & \frac{\delta}{2} & 0 \\ -\frac{1}{2}(1-\frac{\sqrt{3}}{2}\delta) & -\frac{1}{2}\left(\frac{\delta}{2}-\sqrt{3}\right) & 0 \\ 0 & 0 & \frac{c}{a} \end{pmatrix}$$

$$\frac{\Delta\mathrm{E}}{V} = \frac{1}{4}(C_{11} - C_{12})\delta^2$$

*C*33 can be obtained by using the strain *e* = (0, 0, δ, 0, 0, 0):

$$D3 = \begin{pmatrix} 1 & 0 & 0 \\ -\frac{1}{2} & \frac{\sqrt{3}}{2} & 0 \\ 0 & 0 & \frac{c}{a}(1+\delta) \end{pmatrix}$$

$$\frac{\Delta \mathrm{E}}{V} = \frac{1}{2} C_{33} \delta^2$$

Also, C_{44} can be obtained by using the strain *e* = (0, 0, 0, δ, δ, 0):

$$D4 = \begin{pmatrix} 1 & 0 & \frac{\delta}{2} \\ -\frac{1}{2} & \frac{\sqrt{3}}{2} & -\frac{\delta}{4}(1-\sqrt{3}) \\ \frac{c\delta}{2a} & \frac{c\delta}{2a} & \frac{c}{a} \end{pmatrix}$$

$$\frac{\Delta \mathrm{E}}{V} = C_{44} \delta^2$$

Under the condition of hydrostatic pressure, *e* = (δ, δ, δ, 0, 0, 0), the bulk modulus, B $= \frac{2}{9}(C_{11} + C_{12} + 2C_{13} + C_{33}/2)$, is calculated:

$$D5 = \begin{pmatrix} 1+\delta & 0 & 0 \\ -\frac{1}{2}(1+\delta) & \frac{\sqrt{3}}{2}(1+\delta) & 0 \\ 0 & 0 & \frac{c}{a}(1+\delta) \end{pmatrix}$$

$$\frac{\Delta \mathrm{E}}{V} = \frac{9}{2} B \delta^2$$

Therefore, C_{13} is determined.

In this study, firstly 35 sets of $\Delta E/V \sim \delta$ data for each phase were obtained by manual calculations by varying δ from -0.03 to 0.03 in steps of +0.01. These data were recorded and kept .

The value of C_{66} was calculated using the formula below:

$$C_{66} = (C_{11} - C_{12})/2$$

3.3 COMPUTATIONAL DETAILS

3.3.1 CONVERGENCE TESTS (OPTIMIZATION)

We carried out the self – consistent field (scf) calculations to determine basic parameters: kinetic energy cut – off and k-points grid by testing the convergence of total energy with these parameters individually.

K-point optimization

K-point was optimized by using the following values and replacing them in the input file. The values were 4 4 3; 5 5 3; 6 6 4; 7 7 4; 8 8 5; 9 9 6; 10 10 6; 11 11 7; . The input file was run in the terminal using the code:

```
mpirum –np 2 -/qe-6.7/bin/pw.x  <gan.scf.***.in>gan.scf.***.out
```

where *** represents the k-point numbers to optimize.

Energy cut-off (ecutwfc)

The kinetic energy cut-off, ecutwfc (in Ry) determines the size of the plane wave (pw) basis set uses to expand wave function. The value of the kinetic energy cut-off corresponds to the neigbouring interaction in the periodic system. Therefore we have to take the optimum value of this cut-off energy.

The ecutwfc was optimized by replacing the ecutwfc value in the input file with values ranging from 55 to 70 with intervals of 5. The input file was then ran in the terminal using the code:

```
mpirum –np 2 -/qe-6.7/bin/pw.x  <gan.scf.**.in>gan.scf.**.out
```

where ** represents the ecutwfc numbers to optimize

Celldm(1) and Celldm(3)

Celldm(1) and Celldm(3) were gotten from inputing the code:

```
~/qe – 6.7 / bin / cellibrav.x.
```

Alat optimization

The “alat” value was optimized from the vc-relax input file using the code:

```
mpirum –np 2 -/qe-6.7/bin/pw.x  <vc.in>vc.out
```

Below is the input file (gan.scf) after the optimization of k point and ecutwfc

```
&CONTROL
   calculation ='scf',
  prefix='gan'
  pseudo_dir='/media/sf_hex_MECH/PSEUDOPOTENTIALS/',
  outdir='./',
/
```

```
&SYSTEM
   ibrav  =4
   celldm(1)= 6.09198986, celldm(3)= 1.62945453
   degauss    =  0.02
   ecutwfc    =  55
   nat        = 4
   ntyp       = 2
   occupations = "smearing"
   smearing    = "gaussian"
/
&electrons
 mixing_beta = 0.7
 diagonalization='david'
/
ATOMIC_SPECIES
Ga 69.723          Ga.pbe-dn-kjpaw_psl.0.2.UPF
N  14.0067         N.pbe-n-kjpaw_psl.0.1.UPF
ATOMIC_POSITIONS {crystal}
```

```
Ga          0.3333335464       0.6666670929       0.5015965158

Ga          0.6666663536       0.3333328071       0.0015965158

N           0.3333330340       0.6666660680       0.8781654842

N           0.6666668660       0.3333338320       0.3781654842

K_POINTS {automatic}

6 6 4 0 0 0
```

The unit cell of GaN in Wurtzite crystal structure was obtained from the input file above using the code:

```
xcrysden –pwi gan.scf.in
```

3.3.2 COMPUTATIONAL CALCULATIONS OF ELASTIC CONSTANTS

First, we create a script for calculating each primitive vector matrix and ran the script in Quantum ESPRESSO terminal. We obtained our lattice constants (c/a) from previously calculated experimental results from the table below:

TABLE 3.2: Calculated equilibrium lattice constants of studied wurzite semiconductors compared to experimental values.

		GaN
a(Å)	Present	3.19
	Experiment	3.19^{b}
c/a	Present	1.63
	Experiment	$1.627^{b,g}$

[b]*Synchroton EDXD experiment by Xia et al, 1993*

[g]*XAS experiment by Perlin et al, 1992*

For example, for $\frac{\Delta \mathrm{E}}{V} = \frac{1}{4}(C_{11} - C_{12})\delta^2$, its primitive vector matrix after applying the strain e = (0, 0, 0, 0, 0, δ) is

$$\mathrm{D2} = \begin{pmatrix} 1 & 0 & 0 \\ [-\frac{1}{2}\left(1 - \frac{\sqrt{3}}{2}\delta\right)] & -\frac{1}{2}\left(\frac{\delta}{2} - \sqrt{3}\right)] & 0 \\ 0 & 0 & \frac{c}{a} \end{pmatrix}$$

Its input file (create.sh) is given as:

```
#!/bin/bash
for ecut in -0.03 -0.02 -0.01 0.00 0.01 0.02 0.03  ; do
ecut1=`echo $ecut | awk '{print(($1*0.866025-1)*0.5)}'`
ecut2=`echo $ecut | awk '{print($1/2)}'`
ecut3=`echo $ecut | awk '{print(0.866025-($1/4))}'`
sys='gan'
cat> $sys.scf.in << EOF
&control
  calculation ='relax',
  prefix='gan'
  pseudo_dir='/media/sf_hex_MECH/PSEUDOPOTENTIALS/',
  outdir='./',
```

```
/

&SYSTEM

   ibrav  =0

   celldm(1)= 6.09198986,

   degauss     =  0.02

   ecutwfc     =  55

   nat         = 4

   ntyp        = 2

   occupations = "smearing"

   smearing    = "gaussian"

/

&electrons

   mixing_beta = 0.7

   conv_thr = 1.0d-8

/

&ions

ion_dynamics='bfgs'

/
```

```
CELL_PARAMETERS {hexagonal}

 1.0000 $ecut2 0.0000

 $ecut1 $ecut3 0.0000

 0.0000 0.0000 1.62945453

ATOMIC_SPECIES

Ga 69.723          Ga.pbe-dn-kjpaw_psl.0.2.UPF

N  14.0067         N.pbe-n-kjpaw_psl.0.1.UPF

ATOMIC_POSITIONS {crystal}

Ga          0.3333335464       0.6666670929       0.5015965158

Ga          0.6666663536       0.3333328071       0.0015965158

N          0.3333330340       0.6666660680       0.8781654842

N          0.6666668660       0.3333338320       0.3781654842

K_POINTS {automatic}

6 6 4 0 0 0

EOF

 mpirun -np 2 ~/qe-6.7/bin/pw.x < $sys.scf.in > $sys.scf.$ecut.out

 done
```

This script file was ran with the code:

```
#!/bin/bash

for dir in D*; do

cd "$dir" && bash "create.sh"; cd ../;

done
```

D* represents the various primitive vector matrices. The primitive vectors were compared with the manual calculations carried out earlier in section 3.2 of this project work.

This procedure was carried out for all “D”. An “Elastic” script was created for all the various primitive vector matrices for the elastic constants. The unit cell volume gotten from the output files were extracted and recorded in the Elastic script.

For example, for D2 , the unit cell volume was extracted from the output file, gan.scf.0.00.out, and was recorded in the elastic script. The ground state energy, E_0, was chosen to be the final energy in the gan.scf.0.00.out file. Then the following codes were ran in the terminal of the D2 folder:

```
grep Final energy gan.scf.*

grep Final energy gan.scf.* > strain2

sort –n strain2 > strain22

awk ‘{print $1, ($2 + E0)}’ strain22  where E0 is the ground state energy

awk ‘{print $1, ($2 + E0)}’ strain22  > strain222
```

After running these commands, a new input file, strain222, was created. The command, (gnuplot > load ‘elastic’), was used to run the final calculations.

The elastic file was then edited as follows:

```
f(x)=a*x**2+b*x+c

fit f(x) 'strain222' u 1:2 via a, b, c

v=319.0437

# converting Ry/Bohr^3 to GPa

k2=(a*4*14710.5164)/(v)

show variables

plot 'strain222', f(x)
```

The procedure was carried out for all D1, D3, D4, and D5.

CHAPTER FOUR

RESULTS AND DISCUSSION

In this section, we present the structural and mechanical properties of GaN in Wurtzite crystal structure.

4.1 STRUCTURAL PROPERTIES

After successful calculations, the unit cell of GaN in Wurtzite crystal structure is given as:

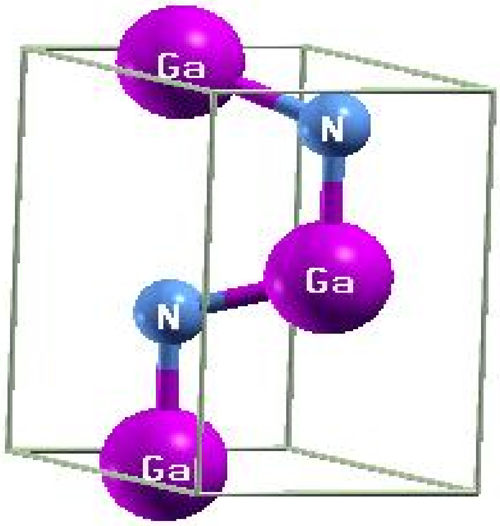

Figure 4. 1: Unit cell of GaN in Wurtzite crystal structure.

From the pictoral representation above, it can be seen that GaN has an hexagonal structure. The bulk modulus determined means that the material can be classified as a hard material.

4.2 MECHANICAL PROPERTIES

We present in this section the mechanical properties of GaN in Wurtzite structure. The mechanical properties consists of elastic constants C_{11} , C_{12}, C_{13}, C_{33}, C_{44}, C_{66} and Bulk modulus, B.

These parameters were calculated using the following expressions:

$$K_1 = C_{11} + C_{12}$$

$$K_2 = C_{11} - C_{12}$$

$$C_{66} = \frac{(C_{11} - C_{12})}{2}$$

$$B = \frac{2}{9}(C_{11} + C_{12} + 2C_{13} + \frac{C_{33}}{2})$$

The values of C_{13}, C_{33}, C_{44} were calculated from computational procedures discussed in section 3.3.2

Table 4.3: Bulk modulus B, and the elastic constants C_{11} , C_{12}, C_{13}, C_{33}, C_{44} and C_{66} (Gpa) for GaN in Wurtzite compared with other calculations and experimental data.

Structure (GaN)	**B (GPa)**	C_{11}	C_{12}	C_{13}	C_{33}	C_{44}	C_{66}
Present work	170.56	311.08	103.21	88.34	353.14	61.62	103.93

DFT	207	367	135	98	409	98	116
Expt[a]	207	346	148	105	389	76	99
Expt[b]	202	367	135	103	405	95	116
Expt[c]	201	366	139	98	403	97	
Expt[d]	210	390	145	106	398	105	122

[a] *DFT(LDA) calculation by Kim et al.*

[b] *DFT(LDA) calculation by Wright.*

[c] *DFT(LDA) calculation by Lepkowski.*

[d] *Brillouin scattering experiment by Polian et al.*

[e] *Synchrotron EDXD experiment by Xia et al.*

From our results (present work), the material is mechanically stable and it meets the stability criterion: $C_{11} > C_{12}, C_{12} > 0, C_{11} + 2C_{12} > 0, C_{44} > 0, C_{11} > \mathrm{B} > C_{12}$ which clearly confirms that the material is stable.

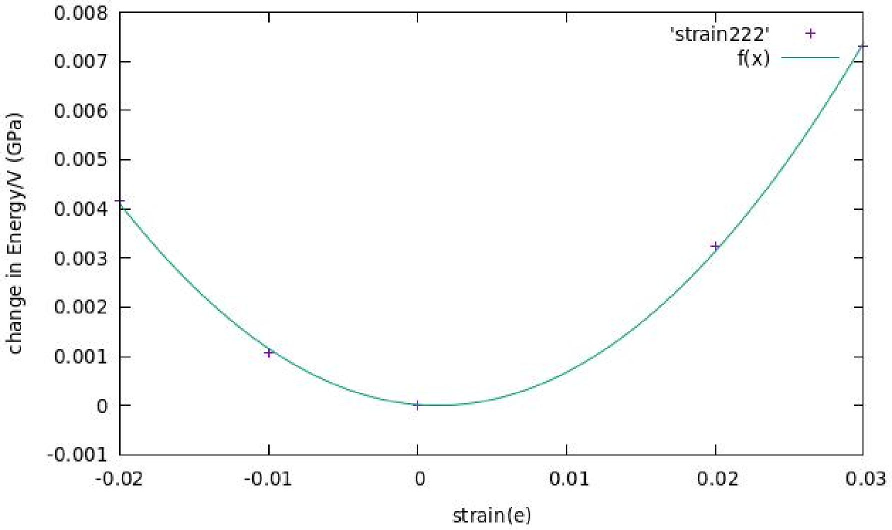
'strain222'
f(x)
change in Energy/V (GPa)
0.008
0.007
0.006
0.005
0.004
0.003
0.002
0.001
0
-0.001
-0.02
-0.01
0
0.01
0.02
0.03
strain(e)

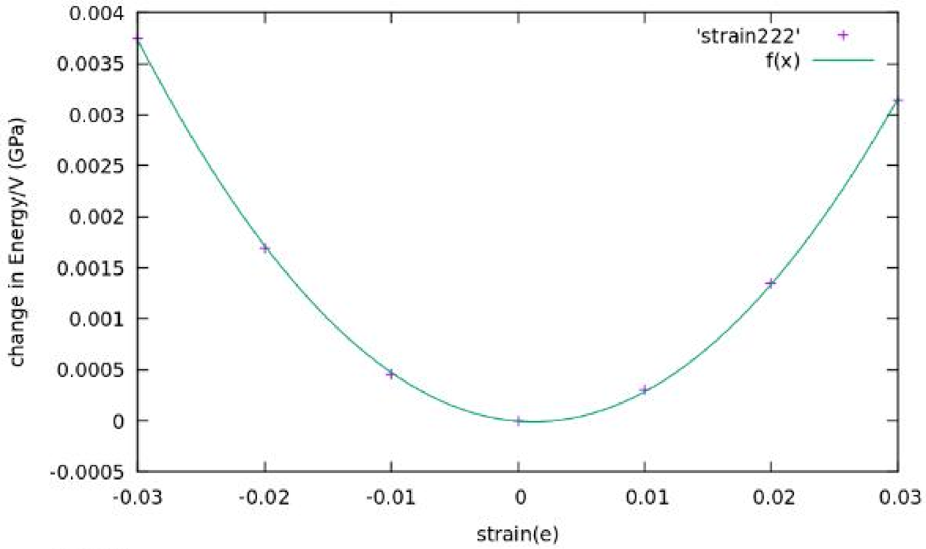
'strain222'
f(x)
change in Energy/V (GPa)
0.004
0.0035
0.003
0.0025
0.002
0.0015
0.001
0.0005
0
-0.0005
-0.03
-0.02
-0.01
0
0.01
0.02
0.03
strain(e)

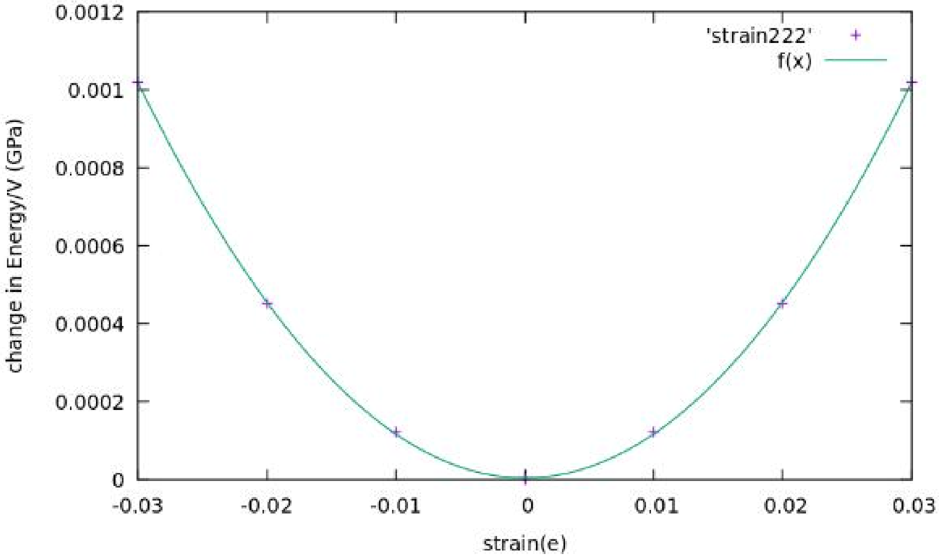
'strain222'
f(x)
change in Energy/V (GPa)
0.0012
0.001
0.0008
0.0006
0.0004
0.0002
0
-0.03
-0.02
-0.01
0
0.01
0.02
0.03
strain(e)

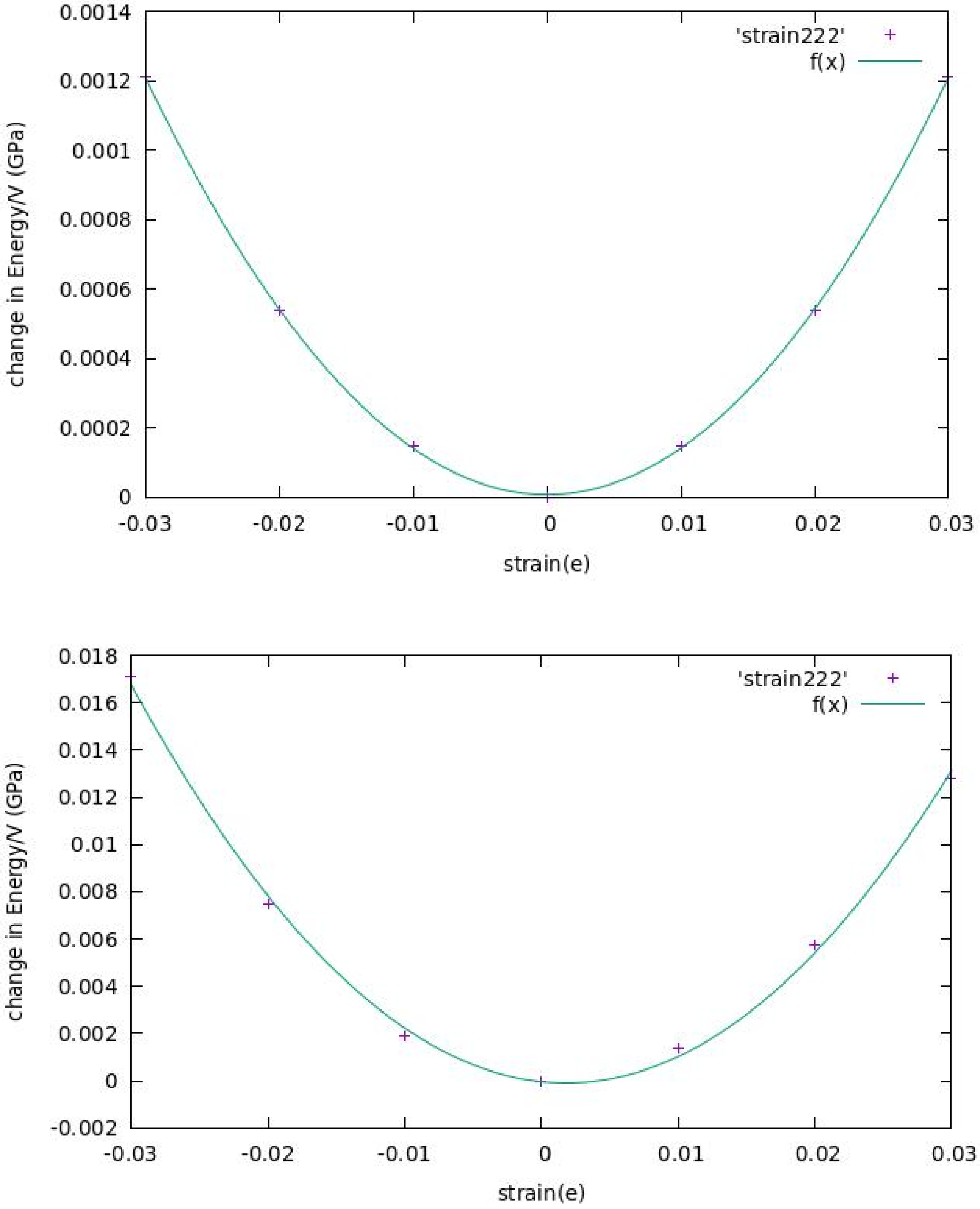

Figure 4.2: The calculation of the elastic constants of Gan from first principle results under various strains: (a) $C_{11} + C_{12}$ (b) $C_{11} - C_{12}$ (c) C_{33} (d) C_{44} (e) bulk modulus, B.

CHAPTER FIVE

FINDINGS AND CONCLUSION

5.0 FINDINGS

From our calculations, we made some findings and they are as follows;

1. that GaN in Wurtzite crystal structure is hexagonal in shape
2. The material satisfies the stability criterion, hence it is mechanically stable and that the material is hard in nature due to its high bulk modulus.

5.1 CONCLUSION

In conclusion, the structural and mechanical properties of GaN in Wurtzite crystal structure have been investigated using first principle calculations and it can be clearly observed that it is hexagonal in structure. The compound also satisfies the mechanical stability criterion, hence it is mechanically stable.

The elastic constants of GaN in Wurtzite crystal structure have been obtained by using first-principles calculations. The reliability of the theoretical data and the calculation procedure are evaluated in detail compared to various experimental results. Overall, good agreement is obtained between theoretical results and calculated experimental results by others in table 4.3.

REFERENCES

"2.4.7.9 The "hot-probe" experiment". ecee.colorado.edu. Archived from the original on 6 March 2021. Retrieved 27 November 2020.

Northrop Grumman, 13 April 2011"Gallium Nitride-Based Modules Set New 180-Day Standard For High Power Operation."

"Kirj.ee" (PDF).

A. Polian, M. Grimsditch, and I. Grzegory, J. Appl. (1996) Phys. 79. 3343

A.F. Wright, J. Appl. (1997) Phys. 82. 2833

Akasaki, I.; Amano, H. (1997). "Crystal Growth and Conductivity Control of Group III Nitride Semiconductors and Their Application to Short Wavelength Light Emitters". Japanese Journal of Applied Physics. 36 (9A): 5393. Bibcode:1997JaJAP..36.5393A. doi:10.1143/JJAP.36.5393.

Amano, H.; Kito, M.; Hiramatsu, K.; Akasaki, I. (1989). "P-Type Conduction in Mg-Doped GaN Treated with Low-Energy Electron Beam Irradiation (LEEBI)". Japanese Journal of Applied Physics. 28 (12): L2112. Bibcode:1989JaJAP..28L2112A. doi:10.1143/JJAP.28.L2112

Arakawa, Y. (2002). "Progress in GaN-based quantum dots for optoelectronics applications". IEEE Journal of Selected Topics in Quantum Electronics. 8 (4): 823 832. Bibcode:2002IJSTQ...8..823A. doi:10.1109/JSTQE.2002.801675.

Askeland, Donald R.; Phulé, Pradeep P. (2006). The science and engineering of materials (5th ed.). Cengage Learning. p. 198. ISBN 978-0-534-55396-8.

Babu, V. Suresh (2010). Solid State Devices and Technology, 3rd Edition. Peason

Beer, Ferdinand P.; Johnston, E. Russell; Dewolf, John; Mazurek, David (2009). Mechanics of Materials. McGraw Hill. p. 56. ISBN 978-0-07-015389-9.

Charles Kittel (1996). op. cit. p. 202. ISBN 978-0-471-11181-8.

Di Carlo, A. (2001). "Tuning Optical Properties of GaN-Based Nanostructures by Charge Screening". Physica Status Solidi A. **183** (1): 81 85. Bibcode:2001PSSAR.183...81D.doi:10.1002/1521-396X(200101)183:1<81::AID PSSA81>3.0.CO;2-N

Feynman, Richard. Feynman Lectures on Physics.

Foster, Corey M.; Collazo, Ramon; Sitar, Zlatko; Ivanisevic, Albena (2013). "abstract NCSU study: Aqueous Stability of Ga- and N-Polar Gallium Nitride". Langmuir. 29 (1): 216 220. doi:10.1021/la304039n. PMID 23227805.

Graeser, S. (2011) Die Wurtzite vom Lengenbach - Polymorphie und Polytypie. Schweizer Strahler: 45: 16-24. [-2H and -4H polytypes].

Green, M. A. (1990). "Intrinsic concentration, effective densities of states, and effective mass in silicon". Journal of Applied Physics. 67 (6): 2944 2954. Bibcode:1990JAP....67.2944G. doi:10.1063/1.345414.

H. Xia, Q. Xia and A. L. Ruoff, (1993).Phys. Rev. B 47, 12925.

Hahn (2002), p. 746, row mC, column Primitive, where the cell parameters are given as a1 = a2, α = β

Hahn, Theo, ed. (2005). International tables for crystallography (5th ed.). Dordrecht, Netherlands: Published for the International Union of Crystallography by Springer. ISBN 978-0-7923-6590-7.

Hanaor, D. A. H.; Assadi, M. H. N.; Li, S.; Yu, A.; Sorrell, C. C. (2012). "Ab initio study of phase stability in doped TiO_2". Computational Mechanics. 50 (2): 185 194. arXiv:1210.7555. Bibcode:2012CompM..50..185H. doi:10.1007/s00466-012-0728 4. S2CID 95958719.

Harafuji, Kenji; Tsuchiya, Taku; Kawamura, Katsuyuki (2004). "Molecular dynamics simulation for evaluating melting point of wurtzite-type GaN crystal". Journal of Applied Physics. 96 (5): 2501. Bibcode:2004JAP....96.2501H. doi:10.1063/1.1772878.

Haynes, William M., ed. (2011). CRC Handbook of Chemistry and Physics (92nd ed.). Boca Raton, FL: CRC Press. p. 4.64. ISBN 1-4398-5511-0.

Hitchcock, Peter B (1988). International tables for crystallography volume A.

Hook, J.R.; Hall, H.E. (2010). Solid State Physics. Manchester Physics Series (2nd ed.). John Wiley & Sons. ISBN 9780471928041.

Johan Strydom; Michael de Rooij; David Reusch; Alex Lidow (2019). GaN Transistors for efficient power conversion (3 ed.). California, USA: Wiley. p. 3. ISBN 978-1-119-59442 0.

Jump up to:[a] [b] Dana, James Dwight; Hurlbut, Cornelius Searle (1959). Dana's Manual of Mineralogy (17th ed.). New York: Chapman Hall. pp. 78–89.

K. Kim, W. R. L. Lambrecht, and B. Segall (1997), Phys. Rev. B 56. 7018

Kittel, Ch. (2004). Introduction to Solid State Physics. John Wiley and Sons. ISBN 0-471-41526-X.

Lidia Łukasiak & Andrzej Jakubowski (January 2010). "History of Semiconductors" (PDF). Journal of Telecommunication and Information Technology: 3. Archived from the original (PDF) on 2013-06-22. Retrieved 2012-08-03.

Lidow, Alexander; Witcher, J. Brandon; Smalley, Ken (March 2011). "Enhancement Mode Gallium Nitride (eGaN) FET Characteristics under Long Term Stress" (PDF). GOMAC Tech Conference.

M. Ueno, M. Yoshida, A. Onodera, O. Shimomura, and K. Takemura, (1994) Phys. Rev. B 49. 14

Mion, Christian (2005). "Investigation of the Thermal Properties of Gallium Nitride Using the Three Omega Technique", Thesis, North Carolina State University.

Morkoç, H.; Strite, S.; Gao, G. B.; Lin, M. E.; Sverdlov, B.; Burns, M. (1994). "Large-band-gap SiC, III-V nitride, and II-VI ZnSe-based semiconductor device technologies". Journal of Applied Physics. 76 (3): 1363. Bibcode:1994JAP....76.1363M. doi:10.1063/1.358463.

Morris, Peter Robin (July 22, 1990). A History of the World Semiconductor Industry. IET. ISBN 9780863412271 – via Google Books.

Neamen, Donald A. (2003). Semiconductor Physics and Devices: Basic Principles (3rd ed.). McGraw-Hill Higher Education. ISBN 0-07-232107-5.

P. Perlin, C. Jauberthie-Carillon, J. P. Itie, A. San Miguel, I. Grzegory, and A. Polian, (1992).Phys. Rev. B 45, 83.

Palache, Charles, Harry Berman & Clifford Frondel (1944), The System of Mineralogy of James Dwight Dana and Edward Salisbury Dana, Yale University 1837-1892, Volume I: Elements, Sulfides, Sulfosalts, Oxides. John Wiley and Sons, Inc., New York. 7th edition, revised and enlarged, pp. 226-228.

Pierret, R. F. (1996). Semiconductor Device Fundamentals. Reading, MA: Addison-Wesley.

Preuss, Paul (11 August 2000). Blue Diode Research Hastens Day of Large-Scale Solid-State Light Sources. Berkeley Lab., lbl.gov.

Prince, E., ed. (2006). International Tables for Crystallography. International Union of Crystallography. doi:10.1107/97809553602060000001. ISBN 978-1-4020-4969-9.

S. P. Lepkowski, J. A. Majewski, and G. Jurczak, (2005)Phys. Rev. B 72. 245201

Shockley, William (1950). Electrons and holes in semiconductors: with applications to transistor electronics. R. E. Krieger Pub. Co. ISBN 978-0-88275-382-9.

Streetman, B. G., & Banerjee, S. K. (2005). Solid State Electronic Devices (6th ed.). Upper Saddle River, NJ: Prentice Hall.

Sze, Simon M. (1981). Physics of Semiconductor Devices (2nd ed.). John Wiley and Sons (WIE). ISBN 0-471-05661-8.

Tang, Shuang; Dresselhaus, Mildred (2012). "Constructing A Large Variety of Dirac-Cone Materials in the BiSb Thin Film System". Nanoscale. 4 (24): 7786 7790. doi:10.1039/C2NR32436A

Tang, Shuang; Dresselhaus, Mildred (2012). "Constructing Anisotropic Single-Dirac-Cones in BiSb Thin Films". Nano Letters. 12 (4): 2021–2026. doi:10.1021/nl300064d.

Terao, S., Iwaya, M.; Nakamura, R.; Kamiyama, S.; Amano, H.; Akasaki, I. (2001). "Fracture of $Al_xGa_{1-x}N$/GaN Heterostructure – Compositional and Impurity Dependence –". Japanese Journal of Applied Physics. 40 (3A): L195. Bibcode:2001JaJAP..40..195T. doi:10.1143/JJAP.40.L195. S2CID 122191162

Togo, Atsushi; Chaput, Laurent; Tanaka, Isao (2015-03-20). "Distributions of phonon lifetimes in Brillouin zones". Physical Review B. 91 (9): 094306. arXiv:1501.00691. doi:10.1103/PhysRevB.91.094306.

Ünlü, Hilmi (September 1992). "A thermodynamic model for determining pressure and temperature effects on the bandgap energies and other properties of some semiconductors". Solid-State Electronics. 35 (9): 1343 1352. Bibcode:1992SSEle..35.1343U. doi:10.1016/0038-1101(92)90170-H.

Zhao, Chao; Alfaraj, Nasir; Subedi, Ram Chandra; Liang, Jian Wei; Alatawi, Abdullah A.; Alhamoud, Abdullah A.; Ebaid, Mohamed; Alias, Mohd Sharizal; Ng, Tien Khee; Ooi, Boon S. (2019). "III-nitride nanowires on unconventional substrates: From materials to optoelectronic device applications". Progress in Quantum Electronics. 61: 1 31. doi:10.1016/j.pquantelec.2018.07.001